Performance of green roof systems

Liu, K. K. Y.; Bass, B.

Performance of green roof systems

Liu, K.; Bass, B.

NRCC-47705

A version of this document is published in / Une version de ce document se trouve dans :
Cool Roofing Symposium, Atlanta, GA., May 12-13, 2005, pp. 1-18

Performance of Green Roof Systems

Karen Liu, National Research Council Canada

Brad Bass, Environment Canada

Global average temperatures have continued to rise as a result of global warming in the past two decades (EPA, nd; Watson et al., 2001). Climate change increases the frequency and intensity of higher temperatures and heat waves. The higher temperatures increase the demand for energy use for air conditioning, increasing greenhouse gas emissions and the levels of other pollutants. This process results in a positive feedback system, whereby the short-term adaptations to a warmer climate, such as increased use of air conditioning, serve to perpetuate global warming and exacerbate other air quality problems. Since high summer temperatures bring about many environmental and health problems (McCarthy et al., 2001), reducing these temperatures has become a major concern for many major metropolitan cities in North America.

Natural landscapes allow for evapotranspiration, a process in which the leaves and the soil convert incoming solar energy into latent heat through the evaporation of water, and prevents it from converting into sensible heat, therefore lowering surface air temperature (Bass, 2001). Vegetation also provides shading and further reduces the surface temperature. On the other hand, in large metropolitan cities, non-vegetated and non-porous surfaces such as roofs, walls, roads and pavement absorb the incoming solar energy and convert it to sensible heat thereby increasing their surface temperatures and the surrounding air temperature. In an urban area with high building density, the increase in the surface temperatures artificially elevates the urban temperature, a phenomenon known as the urban heat island. Therefore, increasing the amount of urban vegetation would lower the citywide air temperature, and help mitigate urban heat island effects (Sailor, 1994). Unfortunately, green spaces are usually limited in urban areas due to the high building density and premium land prices.

Garden roofs, green roofs or rooftop gardens are roofs planted with vegetation. Green roofs add aesthetic appeal to the unused roof space available in most urban areas and provide other multiple benefits. They can reduce a building's energy demand on space conditioning, and hence greenhouse gas emissions, through direct shading of the roof, evapotranspiration and improved insulation values (Minke and Witter, 1982; Liesecke et al., 1989; Christian and Petrie, 1996; Eumorfopoulou and Aravantinos, 1998; Palomo, 1998; Environmental Building News, 2001). The insulation value of a green roof is in both the plants and the growing medium. A 200-mm layer of growing medium and a 200 mm to 400 mm layer of thick grass has a combined insulation value equivalent to 150-mm of mineral wool insulation (RSI 0.14 $m^2 \cdot K/W$ or R 0.79 $h \cdot ft^2 \cdot °F$ /Btu) (Minke and Witter, 1982). Under a green roof, indoor temperatures (without cooling) were found to be at least 3°C to 4°C lower than outdoor temperatures between 25°C and 30°C (Liesecke et al., 1989). A study by Oak Ridge National Laboratory showed that a vegetated roof of 0.46 m to 0.76 m of soil reduced the peak sensible cooling needs of a building by about 25% (Christian and Petrie, 1996). In addition, the green roof did not have a cooling penalty (resistance to heat leaving the building) in the summer like commercial buildings with high roof insulation levels. The National Research Council of Canada showed that an extensive green roof with grass planted on a 150-mm growing medium reduced the heat flow through the roof by over

75% in the spring and summer in Ottawa (Liu and Baskaran, 2003). Also, the roof membrane underneath the green roof rarely went above 30°C compared to an exposed membrane that typically reached over 60°C in the summer. Temperature measurements on an intensive green roof in Singapore showed similar cooling effects (Tan et al., 2003).

Rooftops can become very hot in the summer (Liu and Baskaran, 2003) and it is expected that these hot surfaces will contribute to the urban heat island. Many ways have been proposed to modify the urban surface to mitigate the urban heat island: urban forestry, green roofs and white roofs. A white roof increases the roof albedo, reducing the daytime net energy input. Green roofs convert solar energy into latent heat, through evapotranspiration, as opposed to sensible heat, thus resulting in a cooler surface (Bass, 2001). The lack of vegetation cover has been identified as the most significant contributing factor to the urban heat island phenomenon (Sailor, 1994). Temperature measurements showed that vegetation could reduce the surface temperature and the extent depends on the foliage density (Tan et al., 2003). Given the limited space available for parks and green space in many North American metropolitan cities, placing the vegetation on otherwise unused building rooftops, or green roof technology becomes an attractive solution to mitigate the urban heat island effects.

Background

In 2002, the National Research Council and Environment Canada collaborated to conduct a two-year study on green roof technology with additional financial support from the Technology Early Action Measures (TEAM) program, the City of Toronto, the roofing industry and other stakeholders. The hypothesis was that green roofs not only have the potential to cool a building, but also to mitigate the urban heat island effects and have the potential to cool the city. The City of Toronto was selected for this study because it is the largest municipality in Canada (with a population of about 2.5 million) and is representative of a typical urban center. The National Research Council instrumented an extensive green roof on a community center in Toronto to quantify its thermal performance and stormwater runoff while Environment Canada conducted modeling and simulations to study the ability of green roofs to mitigate the urban heat island effects in Toronto. This paper focuses on the cooling potential of green roofs by presenting supporting field data and simulation findings of this joint study.

Field Monitoring: Thermal Performance of an Extensive Green Roof

Experimental Study

The Eastview Neighbourhood Community Centre sits among low-rise residential and commercial buildings, in Toronto. The green roof was established on top of the gymnasium, which has a low-slope industrial roof (Figure 1). The 460 m^2 roof area was divided length-wise into two sections where two extensive green roof systems were installed (Figure 2). Because of the limited loading capacity, two lightweight extensive green roof systems were selected. The roof of the adjacent mechanical room was used for reference purpose.

The green roof installation was done in several stages due to administrative logistics. Various sensors were embedded in the roofing systems in May 2002. The green roof systems were installed in late July 2002 and sowed with seeds. However, the seeds did not develop well so the

roof was replanted with sedum plugs in the summer of 2003. Therefore, during the observation period reported in this paper (May 2002 – June 2003), the green roof contained very little vegetation (less than 5% coverage). The data provide a baseline comparison for future analysis when the plants have established higher foliage density.

The roofs of the gymnasium and the adjacent mechanical room (Reference Roof) consisted of steel decking, gypsum board, vapor retarder, thermal insulation, fiberboard and modified bituminous membrane. Green Roof System G consists of a composite semi-rigid polymeric drainage and filter mat and a root-anchoring mat. It has 100 mm of lightweight growing medium containing small light-colored granules. Green Roof System S consists of expanded polystyrene drainage panels and a geotextile filter fabric. It has 75 mm of lightweight, dark-colored growing medium containing porous ceramic granules.

The three roof sections were instrumented to measure the temperature profile within and heat flow across the roofing system, soil moisture content and microclimate created by the vegetation and stormwater runoff. A weather station was installed on the rooftop to monitor atmospheric conditions such as temperature, relative humidity, precipitation, solar radiation intensity and atmospheric carbon dioxide concentration. The sensors connect to a data acquisition system, which can be remotely accessed via a modem, for continuous monitoring. Figure 3 shows the major components of the roofing systems and the instrumentation locations.

Results and Findings

Data collection was initiated in May, 2002. The data collected from the first year of monitoring (May 2002 to June 2003) is discussed here with the emphasis on the cooling effects of the green roofs in the summer. Note that the vegetation coverage was minimal during this observation period; therefore, the thermal performance observed was due mainly to the growing medium.

Temperature Profile

Figure 4 shows the temperature profile within the roofing systems on a typical summer day. The membrane on the Reference Roof absorbed solar energy and its temperature rose to 66°C at around 1400 (Figure 4b). The indoor temperature under the ceiling below the Reference Roof (mechanical room) also reached a high of 38°C. The green roofs significantly lowered the roof membrane temperature and delayed the peak (Figure 4c-d). The roof membrane temperature peaked at 38°C at 1830 for Green Roof S and 36°C at 1930 for Green Roof G (Figure 4e-f). The growing medium reduced the heat flow into the building through shading, insulation and evaporative cooling. Because Green Roof G had deeper growing medium, the temperature of the growing medium in S was higher and increased more quickly in comparison to Green Roof G. Since the contributions from the vegetation were minimal, these observations confirm that the deeper growing medium provided extra insulation and thermal mass to the green roof system.

It was also noted that the temperature of the roof membrane in Green Roof G closely followed that of the bottom of the growing medium throughout the day: the difference was less than 1°C across the semi-rigid polymeric drainage mat. On the other hand, for Green Roof S, the temperature difference across the drainage layer was about 4°C with a delay of about two hours most likely due to the additional insulation provided by the expanded polystyrene profile drainage board of Green Roof S.

Temperature Fluctuations

Figure 5 shows the daily temperature extremes experienced by the roof membrane under the green roofs in the first year of observation. The roof membrane was exposed to the elements before the green roofs were installed (before late July 2002). The roof membrane's temperature increased as it absorbed solar energy during the day. As expected, the daily maximum membrane temperature was higher (by about 5°C) for the dark-colored membrane on Green Roof G than the light-colored membrane on Green Roof S. After the green roof systems had been installed, the daily maximum membrane temperature dropped significantly – by about 30°C for Green Roof S (light-colored membrane) and about 40°C for Green Roof G (dark-colored membrane).

The green roofs also reduced the diurnal temperature fluctuation experienced by the roof membrane: from over 50°C to about 10°C in the summer (before and after green roof installation in late July, Figure 5). High temperatures can accelerate the aging process of bituminous membrane while diurnal temperature fluctuations create thermal stresses in the membrane: they affect the long-term performance of the roof membrane and its ability to protect a building from water infiltration. The reduction of the temperature and fluctuations experienced by the roof membrane, due to the green roof technology, will increase the durability of the membrane.

Energy Efficiency

The heat flux through the roof was measured by heat flux transducers (HFT) embedded in the thermal insulation within each roof section (Figure 3). These instruments measure the amount of heat flowing into or out of the building through the roofing system. They were calibrated so that a positive reading represents heat entering the building while a negative reading shows heat leaving the building. The heat flow across the roofing system depends on the temperature difference between the indoor and outdoor temperatures, snow coverage and solar radiation.

On a typical summer day, heat started to enter the building through the Reference Roof not long after sunrise (around 0600), reaching a maximum intensity of about 15 W/m^2 (Figure 6). Heat continued to enter the roofing system until the evening shortly before sunset (around 1800), at which time heat gain changed to heat loss. The green roofs significantly reduced the heat flow (both gain and loss) through the roofing systems to a peak intensity of less than 2.5 W/m^2. Both green roofs lost heat in the morning and did not start to gain heat until the afternoon, near the peak of the solar intensity, indicating that the insulation and thermal mass of the growing media had effectively delayed/reduced heat transfer through the roofing systems (Figure 4a).

Assuming the temperature inside the building was to be kept constant, any heat flow between a building and its environment creates energy demand for space conditioning. Therefore, the energy demand for space conditioning due to the roof can be estimated by the sum of the heat entering and leaving through the roof. The heat flow through the roof was obtained by integrating the heat flux over time or computing the area under the heat flux curve ($kWh/m^2/day$). The positive areas (above the x-axis) represent heat gain and the negative areas (below the x-axis) represent heat loss per unit roof area. Their sum represents the total daily heat flow through the roof. The daily heat flow through the roof section was further averaged over each month to smooth out day-to-day variations. The heat flow data through the three

instrumentation locations on each green roof were averaged to minimize spatial differences across the rooftop.

The normalized average daily heat flows through the roof over the observation period are summarized in Figure 7. Note that the roof membranes on the three roof sections were bare from May to July 2002 before the green roofs were installed. The green roofs consistently reduced the average daily heat flow through the roof throughout the year: more in the summer (70% to 90%) and less in the winter (10% to 30%) again confirming that extensive green roofs can improve the energy efficiency of the roofing system. The green roof was particularly effective in reducing heat gain in the summer. In the first year of monitoring, the green roof reduced the total annual heat gain through the roof by 95% but the heat loss by only 23%.

It is also interesting to note that Green Roof G was more effective in reducing heat flow in the summer but Green Roof S was more effective in the winter. Green Roof G has a deeper growing medium (100 mm) compared to Green Roof S (75 mm). The extra growing medium provided higher insulation, thermal mass and moisture for evaporative cooling to reduce heat gain. However, the effect of the extra insulation was nullified when the growing medium froze in the winter. The expanded polystyrene drainage panel in Green Roof S provided extra insulation, thus improving the energy efficiency in the winter.

The analysis was based solely on heat flow through the roofs; it did not take into account heat flow through the other parts of the building envelope (e.g., walls and windows), which could contribute a much higher fraction of the energy demand of the whole building. Also, the actual dollar saving depends on the type and efficiency of the heating and cooling equipment and the heating/cooling distribution systems, which are building specific.

Computer Modeling: Urban Heat Island and Green Roofs

Modeling the Urban Heat Island

The urban heat island (UHI) has a horizontal scale of several tens of kilometers, roughly two to three times the city size, and it can interact with and modify specific types of atmospheric circulation patterns that operate at a similar or larger scale – the mesoscale in meteorology. To represent the effects at this scale, the Mesoscale Compressible Community Model (MC2) (Benoit et al., 1997) was used to simulate the UHI and the effects of widespread green roof infrastructure. The simulation used a modified version of the Interactive Soil-Biosphere-Atmosphere (ISBA) (Martilli et al., 2005) with the soil-vegetation-atmosphere transfer (SVAT) scheme for the natural area. Detailed parameterization accounts for the drag of buildings on atmospheric flow, turbulent kinetic energy enhancement and sensible heat storage and turbulent fluxes induced by the trapping of infrared and solar radiation in the urban canopy. Energy budgets are considered for roofs, walls, roads and parking lots. The simulated short- and long-wave radiative fluxes also account for the shadowing and multiple reflection of short-wave and long-wave radiation.

Land use distribution data were obtained from available data sets (Kenny et al., 2001). As land use data were not available for the cities that border Toronto, a 10-km band of decreasing urban land use was created for them. Each simulation grid cell was 1 km^2 in Toronto. In this simulation, the green roofs were composed solely of grass. A spatially uniform 50% green roof coverage was introduced that involved the conversion of 50% of the building area into grassland,

equivalent to 5% of the total land use. With the distribution of moisture under irrigation, the percentage of green roofs that actually contributed to the cooling was reduced below the 50% figure as most of the moisture was allocated to those areas that were mostly urban.

Simulation

For this study, MC2 was run over three one-way nested domains. All three domains were 151 by 151 grid points centered on Toronto. The 25 km domain covered much of North America, the 5 km domain the Great Lakes region, and the 1 km domain only the Greater Toronto Area and surrounding area. The base case simulation was performed for a 48-hour period beginning 0000 UTC June 28, 2001. Toronto experienced high temperatures during that week and smog warnings were issued by Environment Canada for five consecutive days beginning June 26. A record for summertime electricity demand in Ontario was set on June 27, the day prior to the beginning of the simulation. The 25 km domain ran for the full 48 hours beginning 0600 UTC, while the subsequent 5 km domain was initialized at 0600 UTC and the 1 km domain at 1200 UTC of the same day. Boundary conditions were provided every six hours for the North American simulation. The 5 km and 1 km domains were each initialized and provided with boundary conditions (at two-hour and one-hour intervals, respectively) by the preceding, coarser domain.

Model Validation

The model temperatures compared well to two Environment Canada weather stations within the City of Toronto, but as there are insufficient observations to assess the whole spatial pattern, the simulation was compared to an earlier UHI analysis for Toronto based on 23 climate stations in and around Toronto from 1964 to 1967 (Munn, 1969). Although the city has grown substantially since 1967, other geographical factors, such as topography and the basic city layout, particularly in the older parts for the city, have not changed dramatically. The simulation for 1400 EDT June 29 modeled temperature distribution was compared to the Munn *et al.*'s distribution of maximum temperatures during the warm season with low wind speeds and both onshore and offshore winds (since the modeled case shows winds nearly parallel or converging near the shoreline).

The comparison is qualitative as previous analysis was based on temperatures at a height of 2 m, while the simulated temperature map is at a height of 5 m, maximum temperatures occur later in the day and any particular day will deviate from a map of average values. In addition, we would expect that the UHI would have grown as the City expanded north, west and east since 1967. Overall, the larger scale features of the modeled temperature distribution appear reasonable when compared to the earlier analysis. In particular, the model reproduced the rapid temperature increase of 2.5-3.5°C over the first 5-10 km inland from the lake, a mean maximum urban temperature located 15-20 km from the shoreline and a ridge of higher maximum temperatures extending north-northwestwards in the offshore observations.

Results and Findings

Simulations were run for three scenarios – base case (BC), irrigated base case (IBC) and irrigated base case with green roofs.

Figure 8 shows the low-level (5 m) temperature and wind distributions at 1400 EDT (1800 UTC) June 29, 2001 output from the base case (BC) simulation. Temperatures in the City of Toronto are 32°C to 34°C, in line with the maximum temperature of 33°C observed at the Toronto international airport weather station. The urban temperature is generally 2° to 3°C warmer in the urban land use region than in the rural areas immediately north and west of Toronto, excluding the area near the lake. The temperature along a 50 km transect running north from downtown Toronto and denoted by a black line in Figure 8 was plotted for several times during the day (Figure 9). Temperature rises rapidly from 1200 EDT to 1400 EDT and the peak urban temperature spreads throughout the city from its noon maximum near the edge of the urban land use. The urban heat island is approximately 2°C and remains constant as temperatures reach their peaks at 1600 EDT and 1800 EDT. During the afternoon period of peak temperature (1400-1800 EDT), the temperature begins dropping toward rural values at a distance of 20 km from downtown, which corresponds to the extent of the urban land use.

Although the temperature pattern along the transect follows an expected UHI pattern, there are some anomalies, for example, the 1°C dip 10 km from the lake at 1400 EDT. This type of anomaly could be due to a strip of urban forest that occurs in this location, the meteorological conditions for that particular day or an error in the land use scheme that was amplified by the urban canyon model used in the simulation. For example, specifying the lowest thermodynamic layer at 10 m introduced a number of other simplifications such as treating the heat, moisture, and momentum fluxes from walls and rooftops as if they originated at the surface and the use of a common wind speed for heat, moisture, and momentum transfer coefficients between the air and roofs, walls, streets.

The irrigated base case (IBC) results in a substantial decrease in temperature as increasing surface moisture increases the latent heat flux, reducing the surface heat flux (and therefore the low-level air temperature). Transects of IBC-BC temperature difference (Figure 10) throughout the day show cooling on the order of 0.5 C to 1°C at all times throughout much of the city, tapering to no difference at the edge of the urban buffer near 30 km to 35 km.

The result of introducing the green roof coverage to the BC scenario is a city-wide cooling of 0.1°C to 0.8 C, with the majority of the strong cooling concentrated near the wind convergence line observed in Figure 8b. To better assess the potential of green roof cooling, irrigation was added to the green roofs to ensure they had sufficient moisture for evapotranspiration. This irrigation scheme resulted in the moisture being located primarily in the commercial and residential high-density areas, reducing the evaporative cooling impact of the green roofs outside the downtown core. The irrigated green roofs reduced the temperature by up to 2°C over the base case and increased the amount of area 1°C cooler or more (Figure 11).

Conclusions

Monitoring of two in-service extensive green roofs in Toronto showed that green roofs are effective in reducing heat gain in the summer, thus providing cooling effects for the buildings. However, they are not as thermally effective in the winter. Although the vegetation was minimal during the first year, these green roofs, with 75 mm to 100 mm of lightweight growing medium, reduced the heat flow through the roof by 70% to 90% in the summer and 10% to 30% in the winter, lowering the energy demand for space conditioning in the building. They also reduced the maximum roof membrane temperature in the summer by more than 20°C and daily

temperature fluctuations experienced by the roof membranes by about 30°C. These reductions will lower the aging and thermal stresses associated with temperature fluctuations, thus contributing positively to membrane durability.

Green Roof G was slightly more effective (about 3% extra) in reducing heat flow in the summer due to its deeper and lighter-colored growing medium. However, Green Roof S was more effective (about 10% extra) in reducing heat flow in the winter due to the extra insulation value in its drainage layer.

Simulation studies using the Mesoscale Compressible Community Model showed that irrigation of the city reduced low-level urban temperatures by 1°C. The addition of irrigated green roofs, located in the downtown area, increased the cooling to 2°C and extended the 1°C cooling region over a larger geographic area. The simulation showed that with sufficient moisture for evapotranspiration, green roofs can play a role in reducing the urban heat island.

Acknowledgement

The authors would like to acknowledge the Technology Early Action Measures, the National Research Council and Environment Canada for their financial and in-kind support. We would like to thank the City of Toronto for providing access and special arrangements to accommodate the research work at the Eastview Neighbourhood Community Centre, in particular to Jim Kamstra, John Minor and Susan Neal of the City of Toronto for providing technical and administrative assistance at the site.

The authors gratefully acknowledge the colleagues at NRC/IRC – Ron Bruce, Ray Demers, Dan Guenter, William Lei and Chris Ladubec – for providing technical help on the instrumentation and data compilation, as well as Bas Baskaran (Group Leader, Performance of Roofing Systems and Insulation) and Ralph Paroli (Director, Building Envelope and Structure Program at IRC) for assistance with the administrative logistics of the project. We would also like to thank Scott Krayenhoff and Alberto Martilli (Department of Earth and Ocean Sciences, University of British Columbia) for the assistance that they provided in simulating the urban heat island and in interpreting the results

References

Bass, B. 2001. “Addressing Urban Environmental Problems with Green Roofs.” *Encyclopedia of Global Environmental Change*, Volume 3. Chichester, UK: John Wiley & Sons.

Benoit, R., M. Desgagne, P. Pellerin, S. Pellerin, Y. Chartier and S. Desjardins. 1997. “The Canadian MC2: A Semi-Lagrangian, Semi-Implicit Wide-Band Atmospheric Model Suited for Fine-Scale Process Studies and Simulation.” *Monthly Weather Review* 125.

Christian, J.E. and T.W. Petrie. 1996. “Sustainable Roofs with Real Energy Savings.” *Proceedings of the Sustainable Low-Slope Roofing Workshop*, ed. A. Desjarlais. Oak Ridge, TN: Oak Ridge National Laboratory, p. 99.

“Environmental Building News.” 2001, November, p.11.

Eumorfopoulou, E. and D. Aravantinos. 1998. "The Contribution of a Planted Roof to the Thermal Protection of Buildings in Greece." *Energy and Buildings* 27: 29-36.

Kenny, W.A, C. Idziak and C. Anderson. 2001: "The Role of Urban Forest in Greenhouse Gas Reduction." Report prepared by W. A. Kenny and Associates.

Liesecke, H-J., B. Krupka and H. Brueggemann. 1989. *Grundlagen der Dachbegruenung Zur Planung, Ausfuhrung und Unterhaltung von Extensivbegruenungen und Einfachen Intensivbegruenungen*. Berlin-Hanover: Patzer Berlag.

Liu, K. and B. Baskaran, B. 2003. "Thermal Performance of Green Roofs through Field Evaluation." *Greening Rooftops for Sustainable Communities,* Chicago.

Martilli, A., A. Clappier and M.W. Rotach. 2002. "An Urban Surfaces Exchange Parameterization for Mesoscale Models." *Boundary-Layer Meteorology* 104: 261-304.

McCarthy, J.K., O.F. Canziani, N.A. Leary, D.J. Dokken and K.S. White, Intergovernmental Panel on Climate Change. 2001. *Climate Change 2001: Impacts, Adaptation, and Vulnerability*. Cambridge, UK: Cambridge University Press.

Minke, G. and G. Witter. 1982. *Haeuser mit Gruenem Pelz, Ein Handbuch zur Hausbegruenung*. Frankfurt: Verlag Dieter Fricke GmbH.

Munn, R. E., M. S. Hirt, and B. F. Findlay, 1969, "A climatological study of the urban temperature anomaly in the lakeshore environment at Toronto" *Journal of Applied Meteorology*, 8:411-422.

Palomo Del Barrio, E. 1998. "Analysis of the Green Roofs Cooling Potential in Buildings." *Energy and Buildings* 27:179-193.

Sailor, D. 1994. "Sensitivity of Coastal Meteorology and Air Quality to Urban Surface Characteristics." Presented at the 74th Annual Meeting of the American Meteorological Society, Nashville, January.

Tan, P.Y., N.H. Wong, Y. Chen, C.L. Ong and A. Sia. 2003. "Thermal Benefits of Rooftop Gardens in Singapore." *Greening Rooftops for Sustainable Communities*. Chicago.

United States, EPA (Environmental Protection Agency). nd. "Global Warming – Climate." <http://yosemite.epa.gov/oar/globalwarming.nsf/content/climate.html>. Accessed February 24, 2005.

Watson, R.T. and the Core Writing Team, Intergovernmental Panel on Climate Change. 2001. *Climate Change 2001: Synthesis Report*. Cambridge, UK: Cambridge University Press.

Figure 1: Growing Medium and Irrigation System Being Installed on the Roof of the Eastview Neighbourhood Community Centre

Green Roof S (dark-colored growing medium) is shown in the foreground while Green Roof G (light-colored growing medium) is shown on the top left.

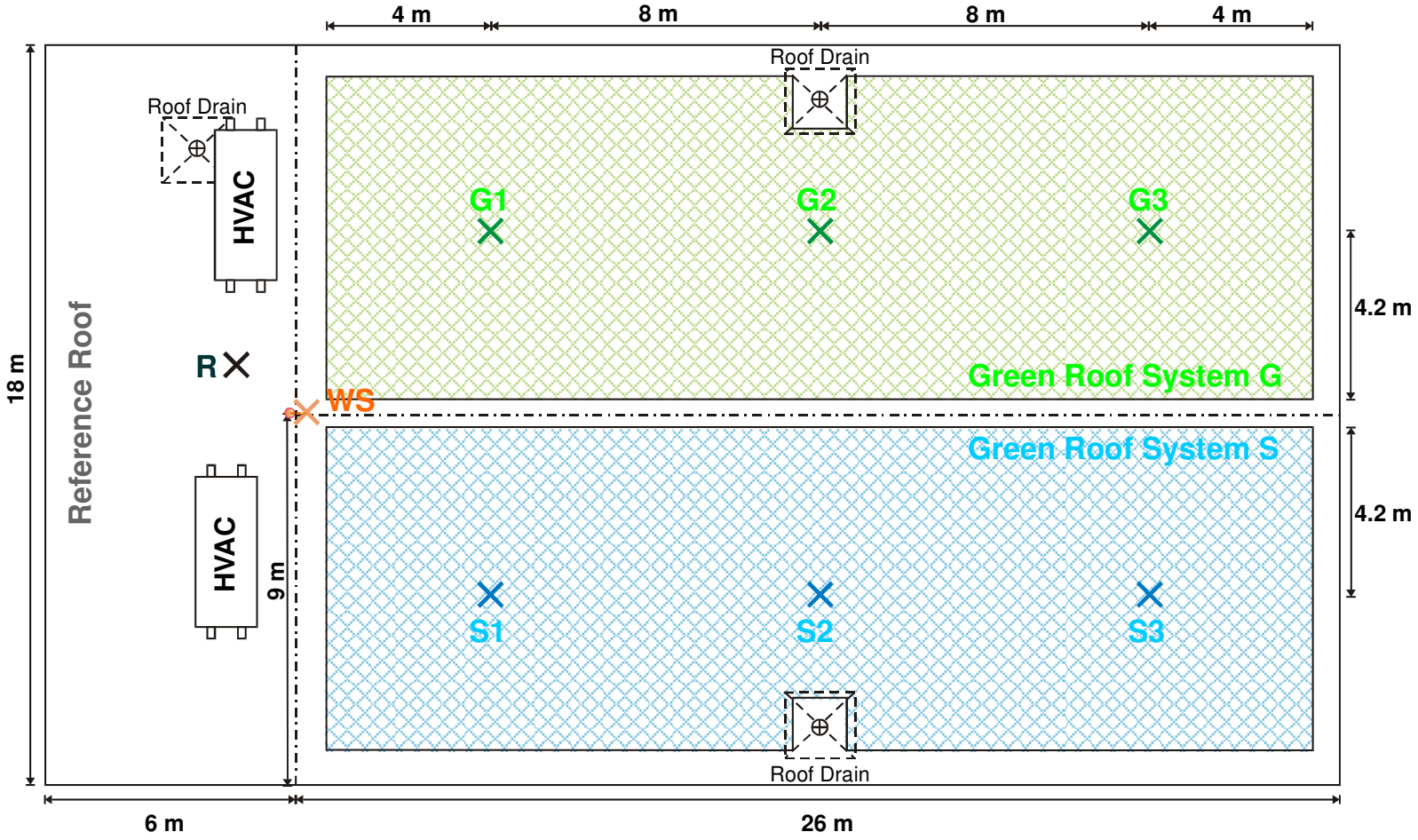

Figure 2: Schematics of the Two Green Roof Systems and the Reference Roof.

The crosses mark the seven instrumentation locations (S1, S2, S3, G1, G2, G2 and R) and the weather station location (WS).

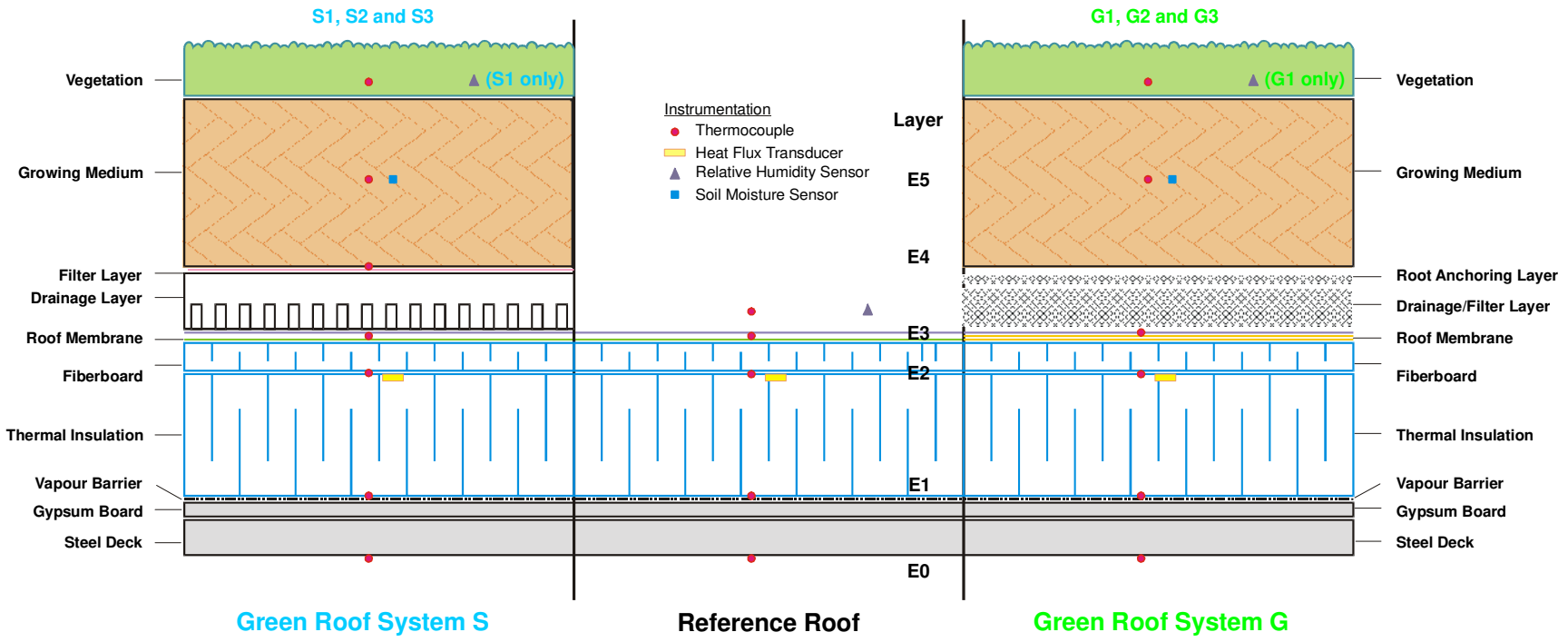

Figure 3: Location of Sensors Embedded Within the Various Roofing Systems at the Eastview Neighbourhood Community Centre (a) Green Roof System S (b) Green Roof System G and (c) Reference Roof.

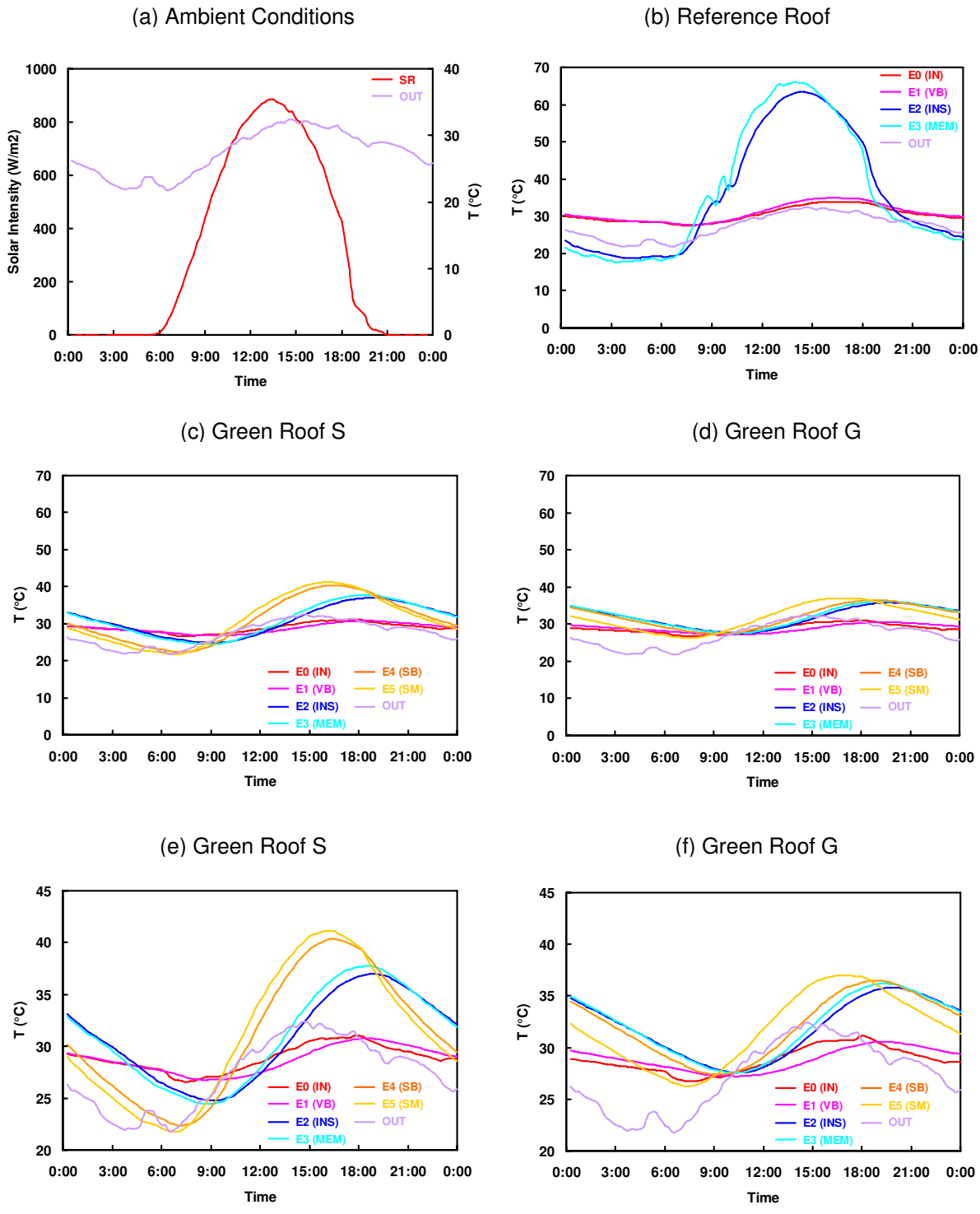

Figure 4: Temperature Profile of the Roof Sections at the Eastview Neighbourhood Community Centre Site on a Typical Summer Day (June 26, 2003).

Refer to Figure 3 for locations of sensors. Note that the temperature scale of green roofs S and G was expanded for clarity in (e) and (f).

(a) Green Roof S

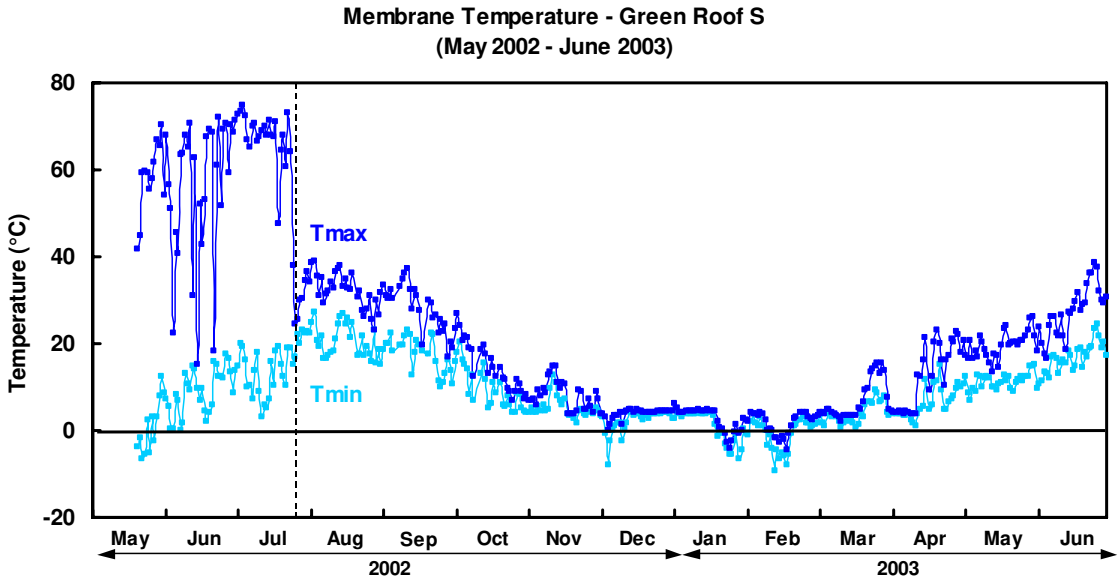

(b) Green Roof G

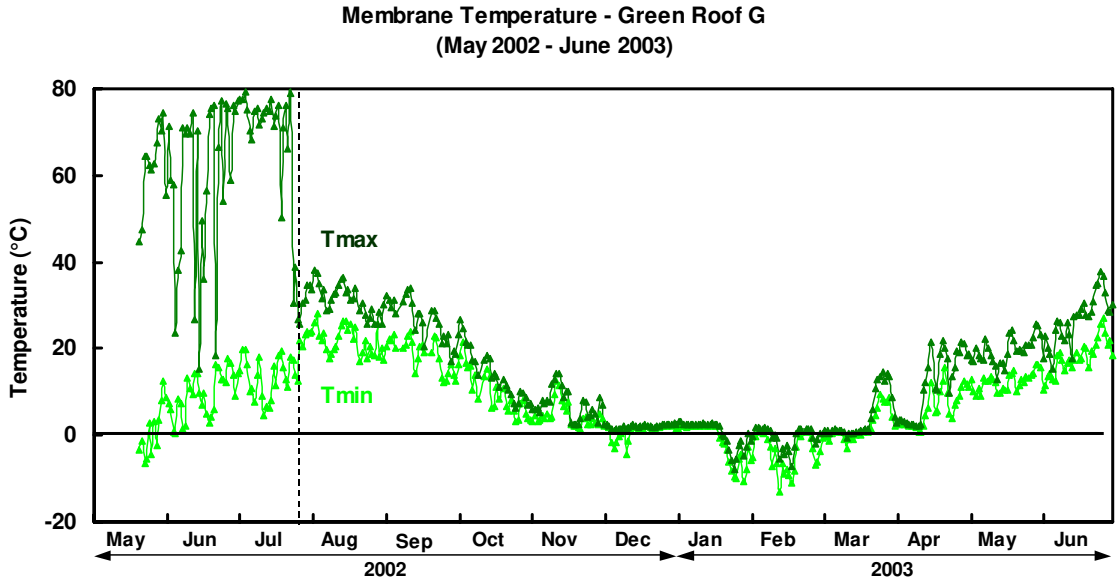

Figure 5: Daily Maximum and Minimum Membrane Temperatures at the Eastview Neighbourhood Community Centre (a) Green Roof S and (b) Green Roof G.

The maximum and minimum temperature values were based on data recorded at three locations (i.e., S1-S3 or G1-G3) on each green roof section. Note that the green roofs were installed in late July 2002.

(a) Reference Roof and Green Roof S

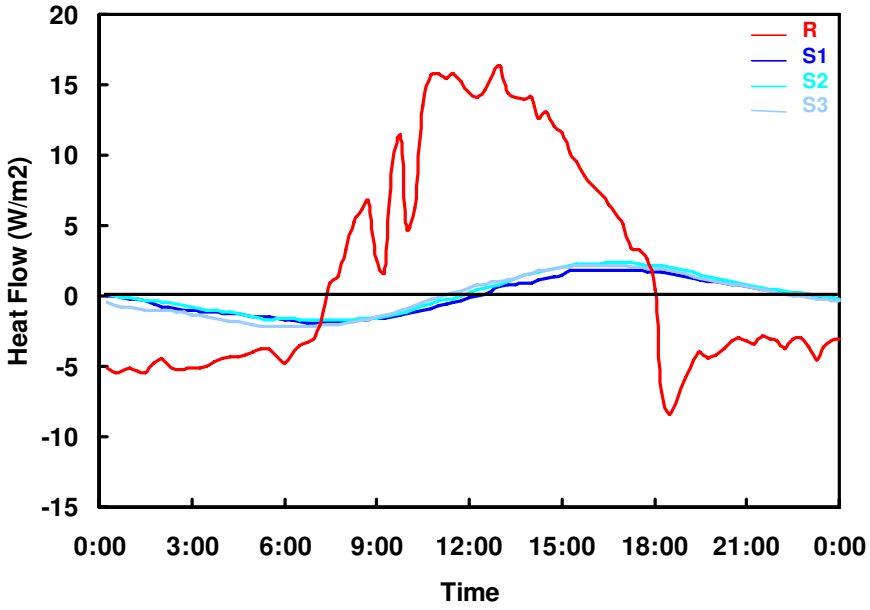

(a) Reference Roof and Green Roof G

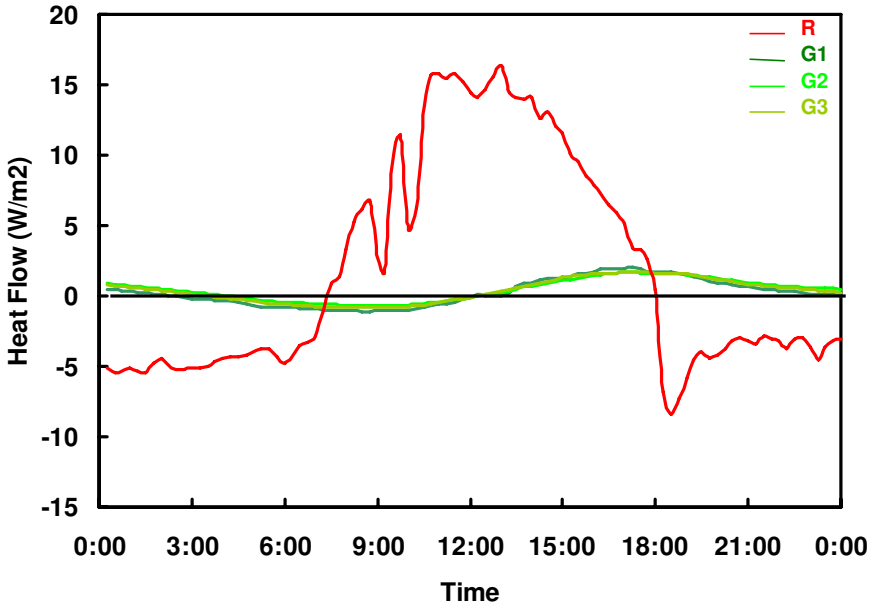

Figure 6: Heat Flow Through the Roof Sections at the Eastview Neighbourhood Community Centre on a Typical Summer Day (June 26, 2003)

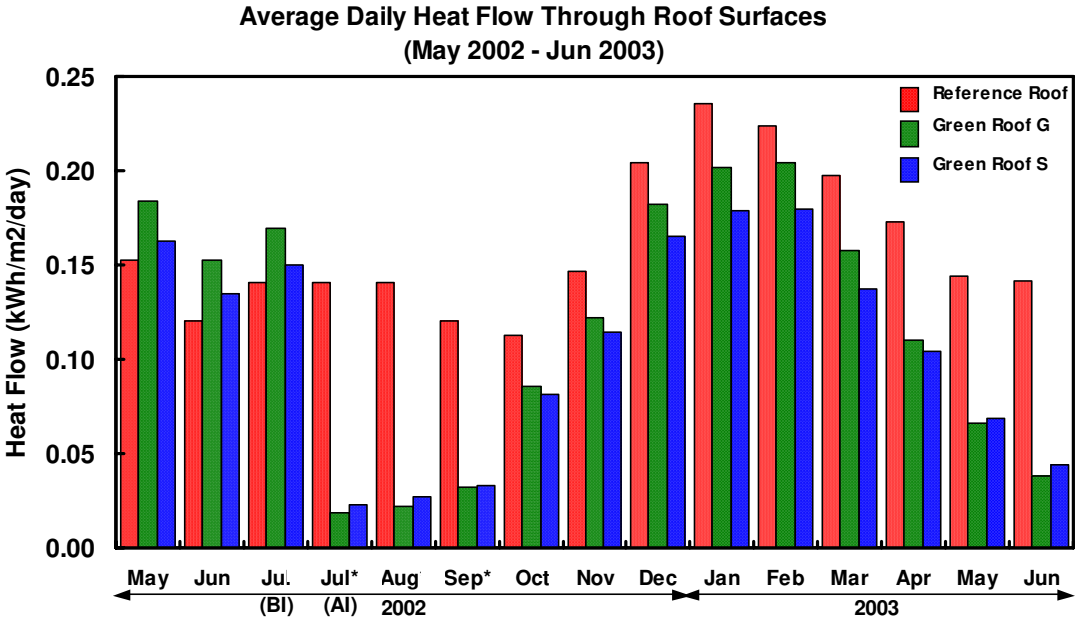

*BI = before installation of green roof, AI = after installation of green roof

Figure 7: Average Daily Energy Demand Due to Heat Flow Through the Roofs at the Eastview Neighbourhood Community Centre.

Note that the green roofs were installed late July 2002.

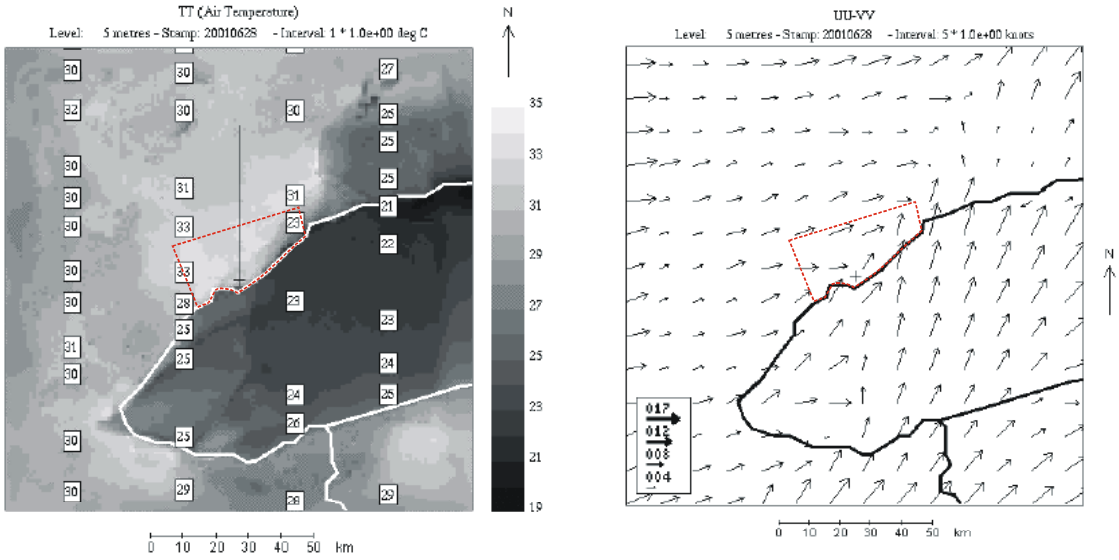

Figure 8: Modeled 5 m (a) Temperature (°C) and (b) Wind (knots) Distributions at 1800 UTC, June 29, 2001 Over the 1 km Simulation Domain.

The solid line denotes the boundary of Lake Ontario and also the Canada-US border south of the lake. Downtown Toronto is located in the center of the image and denoted with a black cross. The reminder of Toronto is to the west, northwest, north and northwest of downtown, marked by the dotted line.

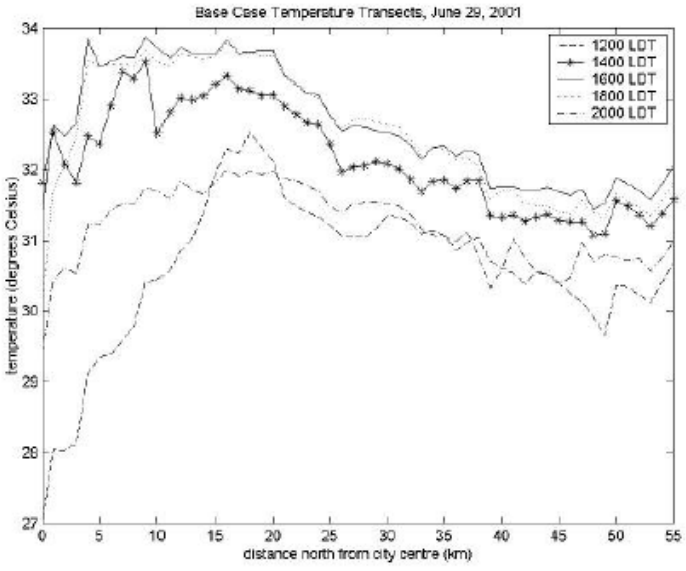

Figure 9: Modeled 5 m Temperature (°C) Plotted vs. Distance North from City Center along the Transect in Figure 8, Five Times During the Afternoon and Evening of June 29

The simulation time corresponding to Figure 8 (1400 EDT) is highlighted with asterisks.

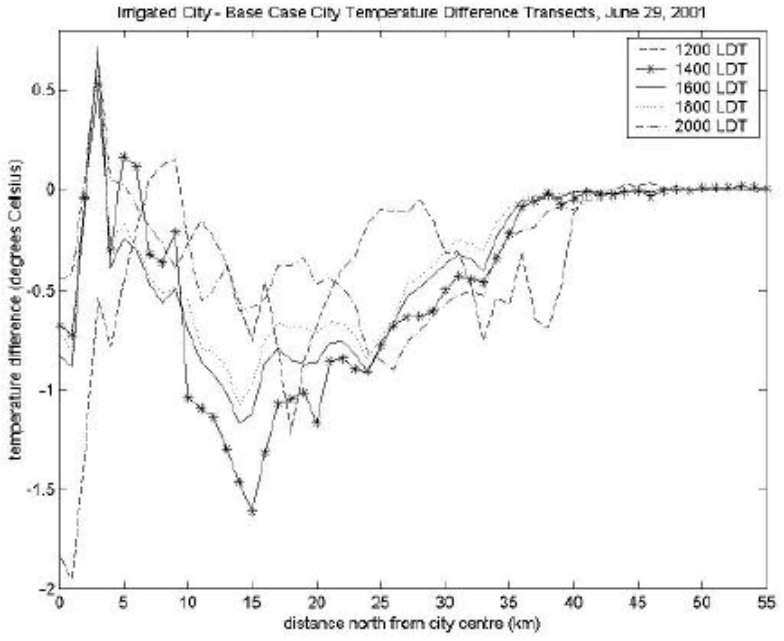

Figure 10: Irrigated Base Case (IBC) Minus the Base Case (BC)

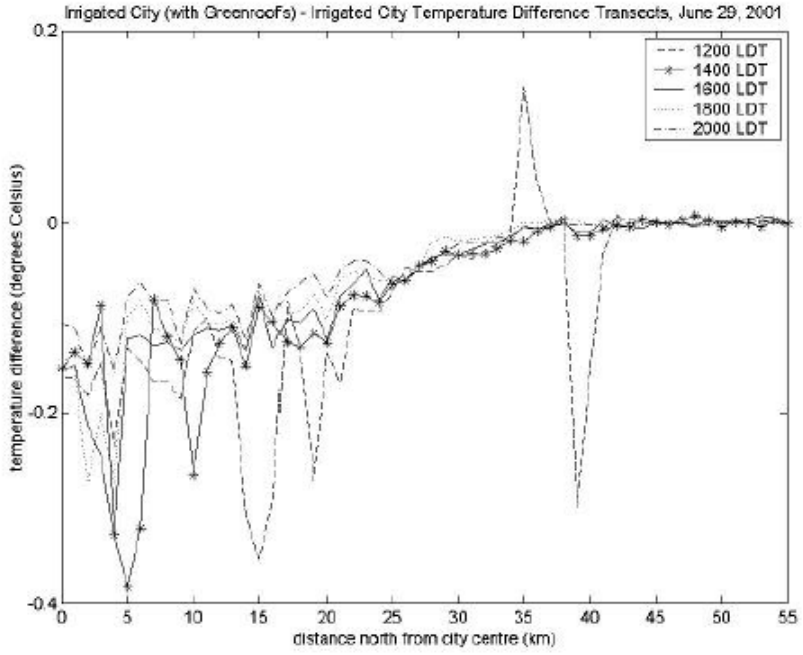

Figure 11: Modeled Temperature Difference at 5 m: Irrigated Base Case with Green Roof Cover Minus the Irrigated Base Case (IBC)